

Formation of Multilayer Polyelectrolyte Complexes by Using Block Ionomer Micelles as Nucleating Particles

Evgeniy A. Lysenko,[†] Pavel S. Chelushkin,[†] Tatiana K. Bronich,[‡] Adi Eisenberg,[§] Victor A. Kabanov,[†] and Alexander V. Kabanov^{*‡}

Department of Polymer Sciences, Faculty of Chemistry, M.V. Lomonosov Moscow State University, Leninskie Gory, V-234, Moscow, 119992, Russia, Department of Pharmaceutical Sciences, College of Pharmacy, University of Nebraska Medical Center, 986025 Nebraska Medical Center, Omaha, Nebraska 68198-6025, and Department of Chemistry, McGill University, 801 Sherbrooke Street West, Montreal, Quebec, Canada H3A 2K6

Received: March 18, 2004; In Final Form: May 14, 2004

This study focuses on the complexes formed between polystyrene-*block*-poly(*N*-ethyl-4-vinylpyridinium bromide) (PS-*b*-PEVP) and poly(sodium methacrylate) (PMANa). These complexes were synthesized as follows. First, PS-*b*-PEVP is dispersed in water, which results in the formation of the micelles with insoluble PS core and cationic PEVP corona. Second, these micelles are reacted with the linear polyanion, PMANa. This leads to formation of the polyion complex micelles that are likely to have the multilayer structure: the PS core surrounded by the intermediate insoluble layer of mutually neutralized polyions and the lyophilizing shell of the polyion that is present in excess. The complexes were characterized by UV and fluorescence spectroscopy, sedimentation velocity, viscometry, static and dynamic light scattering, ζ -potential measurements, and transmission electron microscopy. The properties and stability of the complexes in aqueous dispersion depends on the ratio of charged units of the polycation and polyanion chains, $Z = [\text{PMANa}]/[\text{PEVP}]$. The shell can be either cationic (PEVP) if the polycation is in excess ($Z \leq 0.3$) or anionic (PMANa) if the polyanion is in excess ($Z \geq 1.8$). When Z values are intermediate $0.3 < Z < 1.8$ the micelles become unstable in dispersion and precipitate. At $0.6 \leq Z \leq 1.3$ only the insoluble complexes are formed. Overall, reacting the polyelectrolyte micelles with oppositely charged linear polyelectrolytes represents a simple and effective method of modification of polyelectrolyte micelles and synthesis of micellar dispersions of polyelectrolyte complexes.

Introduction

Interpolyelectrolyte complexes (IPECs) form spontaneously as a result of mixing of oppositely charged polyelectrolytes in aqueous solutions. Previous studies elucidated key factors that influence the kinetics and equilibrium in these reactions, and characterized the structure and properties of resulting IPECs.^{1,2} IPECs have attracted significant attention because they mimic the processes of self-organization in biological systems.³ Furthermore, mixing of oppositely charged polyelectrolytes is a simple and efficient method for synthesis of a broad range of functional polymer materials including DNA–polycation complexes for gene delivery.⁴ Independently the self-assembly of amphiphilic ionogenic block copolymers (block ionomers) in aqueous solutions has been studied intensively.^{5,6} This results in formation of nanoparticles of various structures and shapes, which are primarily determined by the chemical nature and lengths of the ionogenic and nonionogenic blocks.

These two lines of research have recently intersected.^{7–12} It was demonstrated that IPECs containing at least one block ionomer as a component are vastly different from the regular IPECs formed by homopolyelectrolytes or random copolymers of opposite charges. In particular, IPECs formed by the block

ionomers containing nonionic water-soluble block, such as poly(ethylene oxide) (PEO), form stable aqueous dispersions even upon complete neutralization of charges. Diverse materials were synthesized by reacting such block ionomers with oppositely charged synthetic linear polyelectrolytes^{7,8} or block ionomers,⁹ surfactants,¹⁰ DNA,¹¹ or proteins.¹² These materials are sometimes called “block ionomer complexes”^{7,10} or “polyion complex micelles”.¹²

Less is known about the complexes formed by hydrophobic block ionomers containing insoluble nonionic blocks, such as polystyrene (PS). In aqueous solutions such block ionomers form micelles with a core of the insoluble block and a shell of the ionic block.^{13,14} Few studies described complexes of the block ionomer micelles with oppositely charged surfactants and homopolyelectrolytes, which frequently precipitate.^{15–18} This work investigates the IPECs formed by the micelles of PS-*block*-poly(*N*-ethyl-4-vinylpyridinium bromide) (PS-*b*-PEVP) and poly(sodium methacrylate) (PMANa). These IPECs form stable nanoparticles with PS core surrounded by the intermediate insoluble layer of mutually neutralized polyions and the lyophilizing shell of the polyion that is present in excess. By using a combination of potentiometric titration, UV and fluorescence spectroscopy, static light scattering (SLS) and dynamic light scattering (DLS), ζ -potential measurements, sedimentation velocity, and transmission electron microscopy (TEM) techniques the structure and properties of such complexes were characterized.

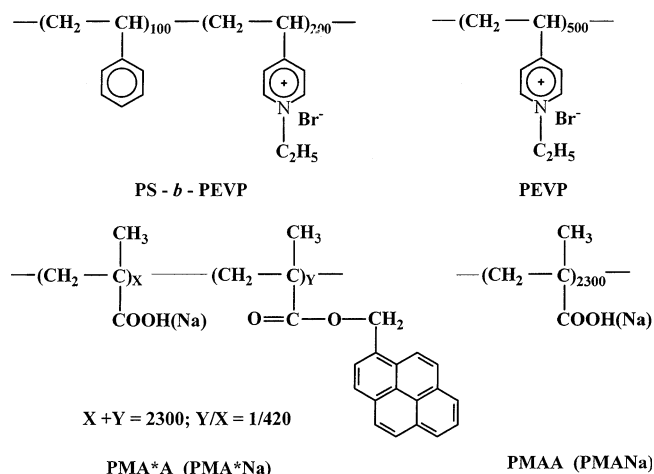
* Address correspondence to this author. Fax: (402) 559-9365. E-mail: akabanov@unmc.edu.

[†] M.V. Lomonosov Moscow State University.

[‡] University of Nebraska Medical Center.

[§] McGill University.

SCHEME 1: Structure of Polymers



Experimental Section

Materials. The structures of the polymers are shown in Scheme 1. PS₁₀₀-*block*-poly(4-vinylpyridine)₂₀₀ (subscript numbers correspond to block lengths) was synthesized by sequential anionic polymerization¹⁹ and then exhaustively modified by ethyl bromide to obtain PS-*b*-PEVP as described before.¹⁶ The degree of modification of the PEVP block was 90% as determined by IR spectroscopy.^{19–21}

Poly(4-vinylpyridine) homopolymer with weight-average molecular mass (M_w) = 50000 g/mol (weight-average degree of polymerization DP_w = 480) was purchased from Poly-sciences, Inc. (Warrington, PA) and exhaustively modified by ethyl bromide to obtain poly(*N*-ethyl-4-vinylpyridinium bromide) (PEVP).¹⁶ The modification degree was 90%.

Poly(methacrylic acid) (PMAA) (M_w = 198000 g/mol, DP_w = 2300) was synthesized by radical polymerization.²² It was also covalently labeled with 1-pyrenyldiazomethane as previously reported.²³ The labeled PMAA (PMA*Na) contained 1 pyrenylmethyl methacrylate group per 420 polymer units. Sodium polymethacrylate (PMANa or PMA*Na) samples were obtained by neutralization of PMAA solutions with sodium hydroxide. The shorter PMAA sample (M_w = 7700 g/mol, DP_w = 90) was from Scientific Polymer Products Inc (Ontario, NY). Aqueous dispersions of PS-*b*-PEVP were prepared by using the dialysis technique as described earlier.¹⁶

Fluorescence Measurements. Fluorescence spectra and intensity measurements were carried out on a Shimadzu RF5000U spectrofluorimeter at λ_{ex} = 339 nm and λ_{em} = 375 nm with a bandwidth of 3 nm for excitation and 1.5 nm for emission, respectively. All measurements were carried out on air-equilibrated solutions at room temperature.

UV Measurements. UV spectra of polymer solutions were recorded on a Shimadzu UV-160 spectrophotometer.

Ultracentrifugation. Sedimentation velocity measurements were performed with a Beckman model E analytical ultracentrifuge equipped with an absorption optical detector at ω = 40000 rpm at room temperature.

Viscometry. The viscosity measurements were performed with an Ubbelohde viscometer at 25 °C. Each sample was equilibrated at least 10 min before measurements.

ζ -Potential and Size Measurements. Electrophoretic mobility measurements were performed on a “ZetaPlus” analyzer (Brookhaven Instrument Co.) with a 30 mW solid-state laser operated at a laser wavelength of 635 nm. ζ -potential of the particles was calculated from the electrophoretic mobility values, using the Smoluchowski equation. Effective hydrodynamic

diameters (D_{eff}) of the particles were measured by photon correlation spectroscopy (DLS) in a thermostatic cell at a scattering angle of 90° using the same instrument equipped with the Multi Angle Sizing Option (BI-MAS). All measurements were performed at 25 °C. Software provided by the manufacturer was used to calculate D_{eff} values. All solutions were prepared with Type 1 water purified by WaterPro PS 90007-00 model (Labconco Co.).

SLS. SLS experiments were performed on a low-angle laser photometer “Chromatix KMX-6/DC” from “Milton Roy” with He-Ne laser operated at a laser wavelength of λ_o = 630 nm and a scattering angle of 6.5°. The values of second virial coefficients (A_2) and weight-average molecular masses (M_w) of PS-*b*-PEVP micelles and IPEC particles were calculated from experimental KC/R_θ vs C dependencies according to Debye’s equation:

$$KC/R_\theta = 1/M_w + 2A_2C$$

where C is weight polymer concentration, $K = (dn/dc)^2 (4\pi^2 n_o^2)/(\lambda_o^4 N_A)$ is the optical constant, R_θ is the Rayleigh ratio, dn/dc is the specific refractive index increment, n_o is the refractive index of the solvent, and N_A is Avogadro’s number. The KC/R_θ vs C dependencies were linear for all species studied. Also, it should be noted that for block copolymers, due to the compositional heterogeneity the M_w and A_2 values are apparent. Specific refractive index increments for PS-*b*-PEVP micelles and IPEC particles in 0.1 M NaCl aqueous solutions were determined by using a differential laser refractometer “Chromatix KMX-16”.

TEM. The negative staining technique was used for the TEM studies. A drop of the sample solution was allowed to settle on a Formvar-coated copper grid for 1 min, the excess of sample was wicked away, and the grid was exposed to 1% uranyl acetate for 20 s. The samples were air-dried and studied with use of a Hitachi H-7000 microscope.

Measurement Error. Relative errors in all measurements reported did not exceed 10%.

Results

Characterization of the PS-*b*-PEVP Micelles. Formation of PS-*b*-PEVP micelles in aqueous dispersions was demonstrated before.¹⁶ The critical micelle concentration (cmc) determined by fluorescence spectroscopy technique, using pyrene as a probe, was 3.0×10^{-3} g/dL (1.14×10^{-4} base-mol/L counting per concentration of charged PEVP units or 5.7×10^{-7} M counting per PS-*b*-PEVP chains).¹⁶ The hydrodynamic and molecular characteristics of the micelles were studied in this work by viscometry, DLS, and SLS. The dependence of the reduced viscosity of the micelles on the copolymer concentration in 0.1 M NaCl was linear suggesting that the polyelectrolyte effect was suppressed. The value of the intrinsic viscosity ($[\eta]$) at this concentration of the salt was 0.41 dL/g. The crossover concentration point (C^*), estimated by using a well-known relationship $C^* \approx 1/[\eta]$, was approximately 2.4 g/dL. Since all experiments described in this work were performed with the concentration range 3.0×10^{-3} g/dL < C ≤ 0.6 g/dL, one can assume that the results refer to the *dilute micelle solutions* and describe the behavior of the individual block ionomer micelles. The effective hydrodynamic diameter of such micelles was 50 to 54 nm. The effective weight-average aggregation number of the PS-*b*-PEVP in the initial micelles was ca. 38 (estimated as the ratio of the apparent M_w of the micelles to the molecular mass of PS-*b*-PEVP = 5.28×10^4 g/mol). This aggregation number was

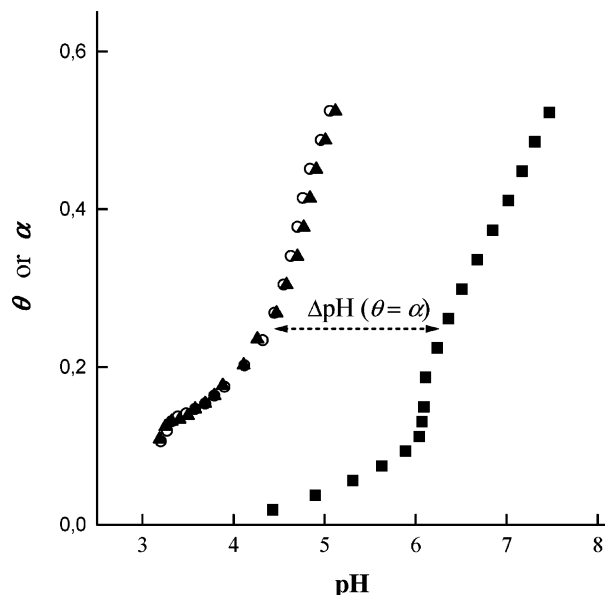


Figure 1. Dependence of θ upon pH in equimolar mixtures of PMAA with PS-*b*-PEVP (\blacktriangle , triangles) or PEVP (\circ , circles) and dependence of α upon pH for the free PMAA (\blacksquare , squares). [PMAA] = [PEVP] = 0.005 base·mol/L; DP_w (PMAA) = 2300.

consistent with the range of the aggregation numbers reported for other block ionomer micelles.^{13,14}

pH Dependence of the Polyion Coupling Reactions. The degree of conversion, θ , in the reactions of PMAA with either PS-*b*-PEVP or PEVP was calculated from the titration curves of PMAA in the presence of these polycations, using mathematical equations proposed earlier.² In the current study we used two samples of PMAA with DP_w = 2300 and 90. Since the results obtained for both samples were mostly similar, here and below we present the data for the longer sample unless it is stated otherwise. Figure 1 presents the dependencies of θ vs pH for the mixtures of PMAA with PS-*b*-PEVP and PEVP, respectively. Both curves were obtained at equivalent molar concentrations of the ionogenic groups of the reacting polyions: $[-\text{PyEt}^+]/([-\text{COOH}] + [-\text{COO}^-]) = 1$. In both cases the θ values increased sharply over the relatively narrow interval of pH 4.5 to 5.0, which was characteristic of the cooperative

polyion binding.² The bends of the curves observed at pH < 4.5 were most likely related to the destruction of the PMAA secondary structures formed under the acidic conditions.^{24,25} This transition was even more clearly displayed in the pH dependence of the ionization degree, α , of the free PMAA at pH 6 (Figure 1). It is noteworthy that for both polycations the θ curves were shifted to lower pH compared to the α curve. The $\Delta\text{pH}(\theta, \alpha) = \text{pH}(\theta) - \text{pH}(\alpha)$ at a given $\theta = \alpha$ was proportional to the differential free energy of cooperative stabilization of IPEC, $\Delta G_{\text{cs}}(\theta, \alpha) = 2.3RT\Delta\text{pH}$.² The θ curves were practically identical, i.e., the free energy contributions were the same for both types of complexes for the entire θ range examined. For example, at $\theta = \alpha = 0.25$, $\Delta G_{\text{cs}}(\theta, \alpha) = 11.1$ kJ/mol. Overall, one can conclude from this study that self-assembly of PEVP chains of the block ionomer within the micelle corona did not alter the ability of these chains to react with the PMAA compared to the homopolymer PEVP.

Characterization of the IPEC Formation with Use of the Fluorescent Probe. To characterize the formation of the IPECs in the pH region when the polyacid was completely ionized (pH 9, $\theta \rightarrow 1$) we used the pyrene-labeled PMA*Na in the form of its salt, PMA*Na. As is shown in Figure 2a the fluorescence intensity of the free PMA*Na linearly increased as the PMA*Na concentration increased. There was little if any effect of the added elementary salt on the free PMA*Na fluorescence. Conversely, in the presence of the PS-*b*-PEVP micelles (added in excess with respect to the polyacid) the fluorescence of the PMA*Na was completely quenched in 0.1 M NaCl solution. It was almost completely restored in 1 M NaCl solution (Figure 2a). This behavior suggested that the IPECs were formed at the lower concentration of the salt. These IPECs disintegrated at the higher concentration of the salt as a result of screening of the electrostatic charges of oppositely charged polyions by small counterions.^{2,26}

In a separate study the PMA*Na was titrated by adding increasing amounts of PS-*b*-PEVP. The progressive quenching of the fluorescence observed in this experiment suggested that IPEC was formed (Figure 2b). It is noteworthy that the fluorescence quenching was complete well below the stoichiometric concentration of the PS-*b*-PEVP. This is probably explained by the strong absorption of the PEVP chains of the

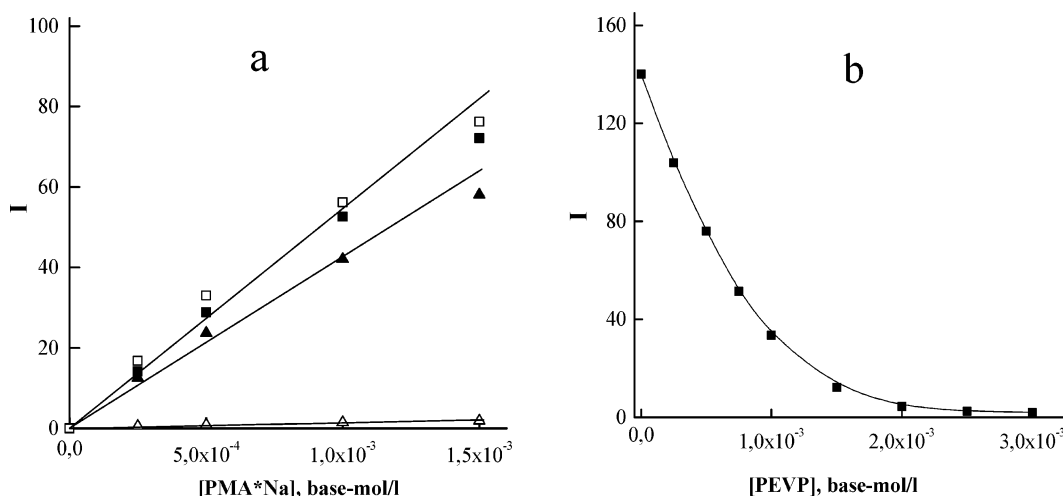


Figure 2. (a) Fluorescence of free PMA*Na in 0.1 M NaCl (\square , open squares) or 1.0 M NaCl (\blacksquare , closed squares) and PMA*Na in mixtures with PS-*b*-PEVP in 0.1 M NaCl (\triangle , open triangles) or 1.0 M NaCl (\blacktriangle , closed triangles). The polycation concentration is constant ([PEVP] = 0.005 base·mol/L), and the polyanion concentration increases. (b) Fluorescence of PMA*Na upon addition of the PS-*b*-PEVP. The polyanion concentration is constant ([PMA*Na] = 0.005 base·mol/L), and the polycation concentration increases. All measurements were carried out on air-equilibrated solutions at room temperature and pH 9. $\lambda_{\text{ex}} = 339$ nm; $\lambda_{\text{em}} = 375$ nm; DP_w(PMA*Na) = 2300.

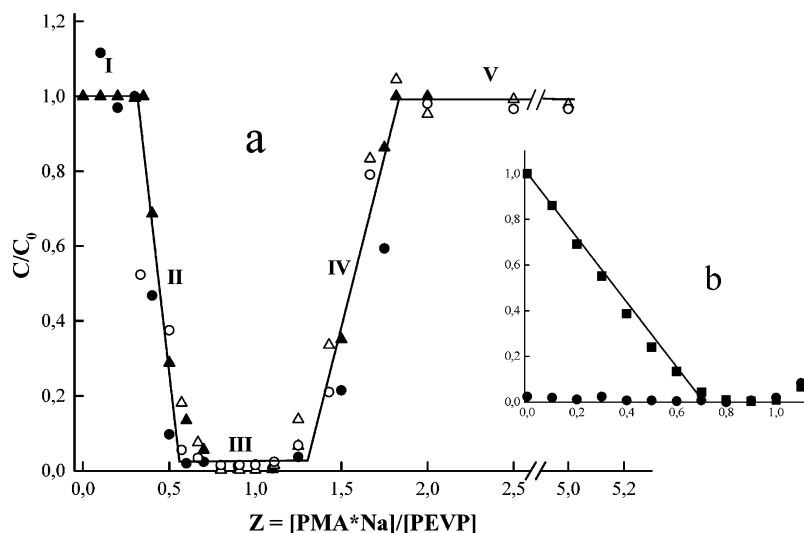


Figure 3. The solubility diagrams of the mixtures of (a) PS-*b*-PEVP and PMA*Na and (b) PEVP and PMA*Na presented as the dependencies of the relative concentrations, C/C_0 , of the polyions remaining in the solution on the composition of the mixtures, Z . (a) The data shown are for PS-*b*-PEVP (\blacktriangle , \triangle , triangles) and PMA*Na (\bullet , \circ , circles). To evaluate the possible effects of the mixing order, the PMA*Na solutions of various concentrations were added to the PS-*b*-PEVP solution of constant concentration $[\text{PEVP}] = 0.005$ base·mol/L (\bullet , \blacktriangle , closed symbols) or vice versa PS-*b*-PEVP was added to the PMA*Na, $[\text{PMA}^*\text{Na}] = 0.005$ base·mol/L (\circ , \triangle , open symbols). (b) The data shown are for PEVP (\blacksquare , squares) and PMA*Na (\bullet , circles). PMA*Na was added to PEVP solution, $[\text{PEVP}] = 0.005$ base·mol/L. (a,b) $[\text{NaCl}] = 0.1$ M; pH 9; $\text{DP}_w(\text{PMA}^*\text{Na}) = 2300$.

block ionomer at the PMA*Na sites containing the hydrophobic pyrenyl groups.²⁶

Solubility Diagram of the PMA*Na/PS-*b*-PEVP Mixtures.

The PMA*Na/PS-*b*-PEVP mixtures were prepared at different compositions, $Z = [\text{PMA}^*\text{Na}]/[\text{PEVP}] = [-]/[+]$, and the precipitates (if formed) were isolated by centrifugation. The concentrations of the polyions remaining in the supernatants were determined by using UV-spectroscopy measurements at $\lambda = 342$ nm (PMA*Na, $\epsilon = 155$ L cm/mol) and $\lambda = 257$ nm (PEVP, $\epsilon = 3040$ L cm/mol). (The extinction coefficients were normalized for the base-molar concentrations of the polyions. The contributions of the UV absorption of PEVP at $\lambda = 342$ nm and the pyrenyl label of PMA*Na at $\lambda = 257$ nm were negligible.) Figure 3a presents the dependencies of the relative amounts of each of the polyions, C/C_0 , on Z . (Here C is the concentration of the polyion remaining in the supernatant and C_0 is the initial concentration of this polyion added to the solution.) This diagram reveals five different regions further designated as I–V. The system was homogeneous and both polymers were quantitatively found in the solution when one of the components was in sufficient excess, specifically, in the regions I ($0 < Z \leq 0.3$ (excess of PEVP)) and V ($Z \geq 1.8$ (excess of PMA*Na)). This suggests that soluble PMA*Na/PS-*b*-PEVP IPECs were formed in these regions. In region III, $0.6 \leq Z \leq 1.3$ both components quantitatively precipitated, suggesting that insoluble IPECs were formed as a result of neutralization of the polyion charges. In this region the composition of the insoluble IPEC approximated Z . The soluble and insoluble IPECs coexisted in the two “transitional” regions II ($0.3 < Z < 0.6$) and IV ($1.3 < Z < 1.8$). Significantly, the C/C_0 values in the entire range of Z practically did not depend on the order of the mixing of the polyion components, i.e., either PS-*b*-PEVP micelle solution was added to the PMA*Na solution (Figure 3a, open symbols) or vice versa (Figure 3a, closed symbols). This suggested that all the transitions observed in the studied system were reversible. This also implied that in areas II and IV the soluble and insoluble IPECs coexisted in thermodynamic equilibrium.

Under the similar conditions the mixtures of PMA*Na and linear PEVP displayed very different behavior (Figure 3b). In

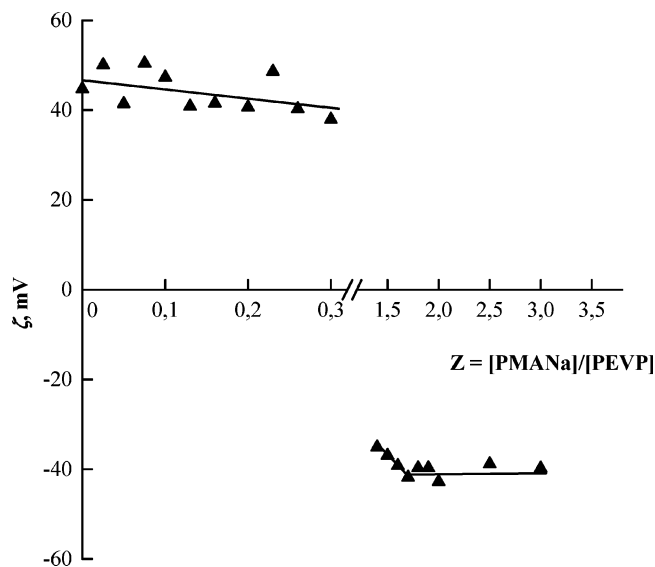


Figure 4. Dependence of ζ -potential of the PMANa/PS-*b*-PEVP IPECs on Z . $[\text{PEVP}] = 0.001$ base·mol/L; $[\text{NaCl}] = 0.01$ M; pH 9; $\text{DP}_w(\text{PMANa}) = 2300$.

this case in the entire range of $Z \leq 1$ only the insoluble complex was formed. At $0 < Z \leq 0.7$ this complex was of practically constant composition (ca. 0.7, i.e., contained ca. 30 mol % excess of the PEVP units). At $0.7 < Z < 1$ the complex remained insoluble but the composition increased and reached the stoichiometry at $Z = 1$. At $Z > 1$ this complex was ultimately dissolved suggesting that some excess of the added PMA*Na chains incorporated in the IPEC resulting in its solubilization (not shown in the figure).

ζ -Potential of the PMANa/PS-*b*-PEVP Complexes. Figure 4 presents the dependence of the ζ -potential of the soluble PMANa/PS-*b*-PEVP complexes formed at $Z \leq 0.3$ and $Z > 1.4$. At $Z \leq 0.3$ the complexes were positively charged, i.e., contained an excess of PEVP compared to PMANa. At $Z > 1.4$ the complexes were negatively charged, i.e., contained an excess of PMANa compared to PEVP. At $Z \geq 1.8$ the ζ -potential of the particles leveled off (ca. -40 mV), indicating

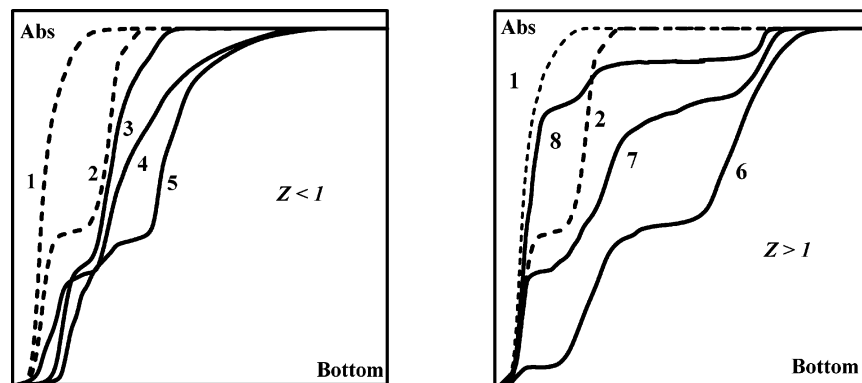


Figure 5. Sedimentation profiles of PMA*Na (1), PS-*b*-PEVP (2), and PMA*Na in PMA*Na/PS-*b*-PEVP mixtures (3–8). The scanning wavelengths were 342 nm (1, 3–8) or 294 nm (2). The *Z* values were 0.15 (3), 0.2 (4), 0.3 (5), 2.0 (6), 5.0 (7), and 10.0 (8). The concentrations of the polyions were the following: (1, 6–8) [PMA*Na] = 0.005 base·mol/L, (2) [PEVP] = 0.01 base·mol/L, (3–5) [PEVP] = 0.005 base·mol/L. Other conditions were [NaCl] = 0.1 M, pH 9, ω = 40000 rpm, and (1) *t* = 11 min, (2, 4) *t* = 15 min, (3) *t* = 13 min, (5, 8) *t* = 17 min, (6) *t* = 16 min, and (7) *t* = 18 min.

that the limit in incorporation of PMANa in IPEC was reached. Clearly, this study suggests that at the excess of the polycation the IPEC particles had a positively charged corona of the PEVP chains that were not neutralized by the polyanion. Conversely, at the excess of the polyanion IPEC particles with the negatively charged PMANa corona were formed.

Characterization of Dispersed IPECs by Ultracentrifugation. Figure 5 presents the scan sedimentation profiles of PMA*Na ($\lambda_{\text{scan}} = 342$ nm), PS-*b*-PEVP ($\lambda_{\text{scan}} = 294$ nm), and their mixtures ($\lambda_{\text{scan}} = 342$ nm). The free PMA*Na (curve 1) represented a single fraction, 5 Sv, while the PS-*b*-PEVP (curve 2) exhibited bimodal distribution with two types of species, 8 and 21 Sv. The reasons for the appearance of two types of micelle-like species in PS-*b*-PEVP dispersions were discussed earlier.¹⁶ The profiles for the PMA*Na/PS-*b*-PEVP mixtures at the block ionomer excess (*Z* = 0.15, 0.2, and 0.3) were also bimodal, i.e., the PMA*Na was quantitatively bound to each of the PS-*b*-PEVP species resulting in two distinct IPEC fractions (curves 3, 4, and 5). The higher the *Z* was, the more PMA*Na was bound to these IPECs, and the greater the IPEC sedimentation coefficients were (e.g., 13 and 23 Sv at *Z* = 0.15 to 15 and 32 Sv at *Z* = 0.3). At the PMA*Na excess (*Z* = 2.0, 5.0, and 10.0) the sedimentation coefficients reached the constant values of 20 and 40 Sv, while the excess of free PMA*Na that did not incorporate in the IPEC appeared as a separate fraction, 5 Sv. The analysis of the profiles of the PMA*Na/PS-*b*-PEVP mixtures registered at $\lambda_{\text{scan}} = 294$ nm (not shown) suggested that PS-*b*-PEVP quantitatively incorporated in the IPEC at every *Z*. Figure 6 presents the plot of the relative amounts of the free PMA*Na in equilibrium with the IPEC in the range of PMA*Na excess as a function of 1/*Z*. The linear character of this dependence at 1/*Z* < 0.54 (approximately *Z* > 1.8) implies that the composition of the IPEC remained constant and was ca. 1.8 (the point of intercept with the abscissa). Overall, there was a limit for the amount of PMA*Na incorporated into IPEC, corresponding to approximately 2-fold excess of PMA*Na units compared to PEVP units. This result was consistent with the leveling-off of the ζ -potential values at ca. *Z* > 1.8.

Morphology and Molecular Characteristics of Soluble PMANa/PS-*b*-PEVP IPECs. Figure 7 presents TEM micrographs of the initial PS-*b*-PEVP micelles and PMANa/PS-*b*-PEVP IPEC particles formed at *Z* = 0.15 and 1.75. For both the initial micelles and IPECs the TEM images revealed two types of spherical particles with the average diameters of ca. 28 and 13 nm. The effective hydrodynamic diameters (D_{eff}) of the PMANa/PS-*b*-PEVP complexes were determined by using

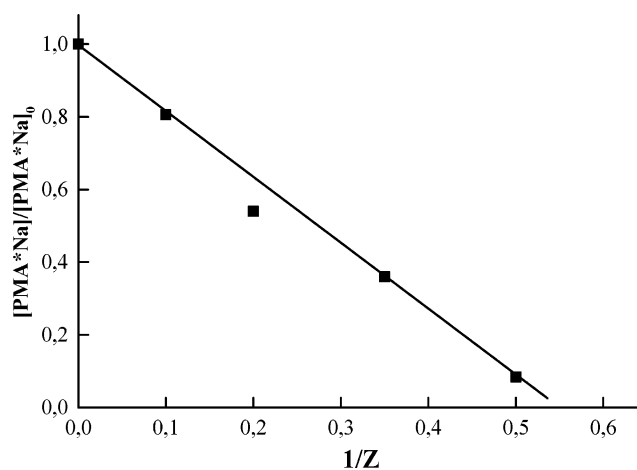


Figure 6. The dependence of the fraction of the free PMA*Na on 1/*Z*. The ratios of the free and total PMA*Na in the system, [PMA*Na]/[PMA*Na]₀, were determined based on the sedimentation profiles recorded at the PMA*Na excess. [PMA*Na]₀ = 0.005 base·mol/L. [NaCl] = 0.1 M; pH 9; DP_w (PMA*Na) = 2300.

DLS. As the values of *Z* increased within the range 0 < *Z* < 0.3 the D_{eff} values first slightly increased and then leveled off at ca. 60 nm. At ca. *Z* > 1.7 the D_{eff} values were practically constant, ca. 65 nm. The sizes of the particles calculated from the TEM data were less than those determined by the DLS. This was not surprising, since in contrast to DLS the TEM images were obtained in the absence of the solvent. Table 1 presents the refractive index increments, dn/dc , the second virial coefficients, A_2 , the apparent M_w and aggregation numbers, N_w (determined by SLS), and D_{eff} (determined by DLS) for the PS-*b*-PEVP micelles and PMANa/PS-*b*-PEVP complexes (*Z* = 0.15 and 1.75). Since the sedimentation and TEM studies revealed two types of polymer micelles in the system the values of D_{eff} , M_w , and N_w reported in Table 1 are average for all types of aggregates present in the system. The similarity in morphology (Figure 7) and molecular properties (Table 1) between PS-*b*-PEVP micelles and positively or negatively charged PMANa/PS-*b*-PEVP IPEC particles seems to be remarkable. It strongly suggests that only one original block ionomer micelle incorporates into IPEC nanoparticles and the PS cores remain unchanged, i.e., no disaggregation, fusion, or flocculation of the original PS-*b*-PEVP micelles occur once the complexes are formed. Overall, this study suggested that the morphology and molecular characteristics of the dispersed IPEC were imposed

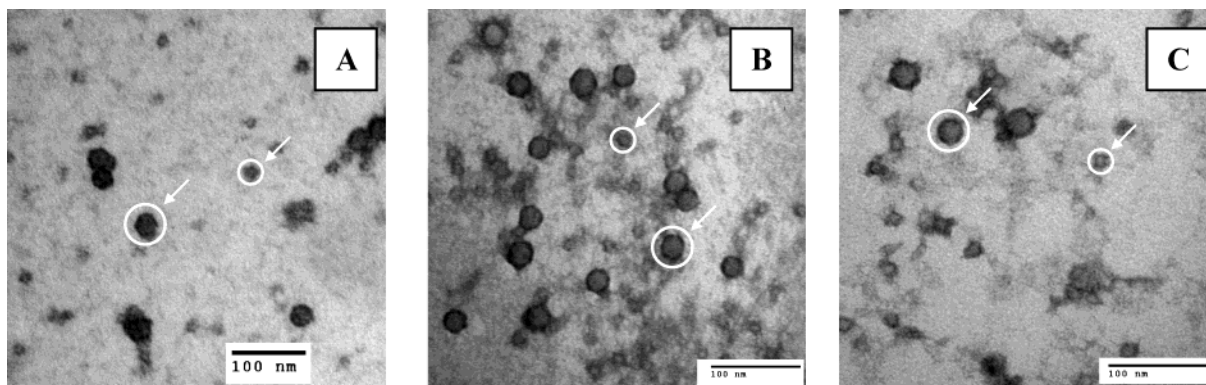


Figure 7. TEM images of PS-*b*-PEVP micelles (A) and PMANa/PS-*b*-PEVP IPECs at $Z = 0.15$ (B) and 1.75 (C). [PEVP] = 0.001 base·mol/L; [NaCl] = 0.01 M; pH 9. White circumferences and arrows show two types of spherical particles.

TABLE 1: Molecular Characteristics of PS-*b*-PEVP Micelles and Particles of PMANa/PS-*b*-PEVP IPEC in 0.1 M NaCl Based on SLS and DLS Measurements

Z	dn/dc , mL/g	A_2 , mol L/g ^a	M_w , g/mol	N_w	D_{eff} , nm
0	0.2038	-7.7×10^{-5}	2.02×10^6	38	50
0.15	0.2265	-5.0×10^{-5}	2.08×10^6	39	60
1.75	0.2220	-5.3×10^{-5}	2.40×10^6	35	65

^a Low A_2 values observed in this study are consistent with the earlier reports that A_2 values for block ionomer micelles are close to zero.^{13,27}

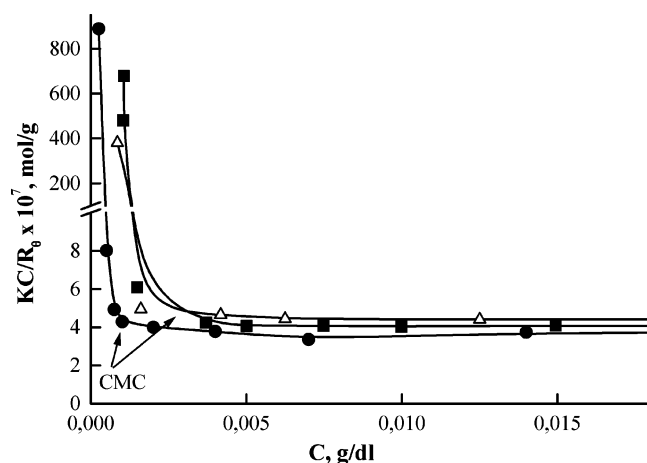


Figure 8. Dependence of KC/R_θ on the block ionomer or complex concentration (C) for solutions of the free PS-*b*-PEVP (Δ , triangles) and PMANa/PS-*b*-PEVP mixtures at $Z = 0.15$ (\blacksquare , squares) and 1.75 (\bullet , circles). [NaCl] = 0.1 M; pH 9; $DP_w(\text{PMANa}) = 2300$. Arrows designate the CMC points.

by the morphology and molecular characteristics of the original PS-*b*-PEVP micelles.

Determination of CMC of IPEC by SLS. The dependencies of the Rayleigh ratio, R_θ , on the block ionomer concentration measured for PS-*b*-PEVP alone and for the PMANa/PS-*b*-PEVP mixtures ($Z = 0.15$ and 1.75) displayed characteristic points corresponding to the onsets of the progressive increase of R_θ that were indicative of CMC (data not shown). The micellization behavior was also clearly evident from the dependence of the value of KC/R_θ vs concentration of PS-*b*-PEVP, which revealed a sharp decrease at concentrations below CMC and practically leveled off above the CMC (Figure 8). The estimate of the CMC obtained from the SLS data for the PS-*b*-PEVP alone was 2.7×10^{-7} M, which was in reasonable agreement with 5.7×10^{-7} M previously determined with the fluorescence spectroscopy technique.¹⁶ The values of CMC for the PMANa/PS-*b*-PEVP mixtures ($Z = 0.15$ and 1.75) were 2.7×10^{-7} and 7.3×10^{-8} M, respectively.

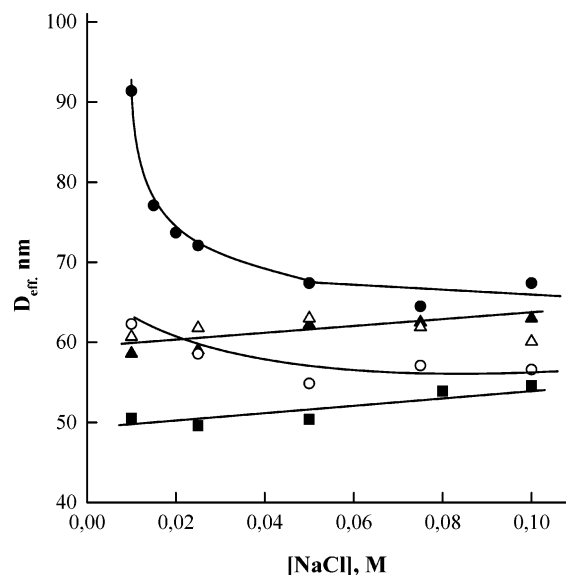


Figure 9. Dependence of D_{eff} on the NaCl concentration for the PS-*b*-PEVP micelles (\blacksquare , squares) and PMANa/PS-*b*-PEVP IPECs at $Z = 0.15$ (\blacktriangle , triangles) and 1.75 (\bullet , circles). Two samples of PMANa were used with $DP_w = 2300$ (\blacktriangle , closed symbols) and 90 (\triangle , open symbols). [PEVP] = 0.001 base·mol/L; pH 9.

Polyelectrolyte Effect in the IPEC Systems. Figure 9 presents the dependencies of the D_{eff} of PS-*b*-PEVP micelles and PMANa/PS-*b*-PEVP IPECs upon the NaCl concentration. As is seen in the figure the diameters of the PS-*b*-PEVP micelles remained practically constant within the NaCl concentration range of 0.01 to 0.1 M. Similar behavior was observed for PMANa/PS-*b*-PEVP IPEC (PMANa $DP_w = 2300$ and 90) at the excess of the polycation, $Z = 0.15$ underscoring the similarity of such complexes with the PS-*b*-PEVP micelles. The absence of the polyelectrolyte effect in this system was evidently explained by the relatively short length of the polycation chains forming the corona of the particles. Quite different behavior was displayed by the IPEC at the excess of the polyanion ($Z = 1.75$). Specifically, increasing the salt concentration was accompanied by a gradual decrease of D_{eff} , suggesting a pronounced polyelectrolyte effect exhibited by the PMANa ($DP_w = 2300$) corona. This effect was much less pronounced when the short PMANa ($DP_w = 90$) was used instead of the long PMANa ($DP_w = 2300$). This result can be explained by the presence, in the outer layer of the IPEC, of a significant amount of the free fragments of the polyelectrolyte added in excess, i.e., formation of the polyelectrolyte corona. Notably, as the polymerization degree of the excessive polyelectrolyte increases

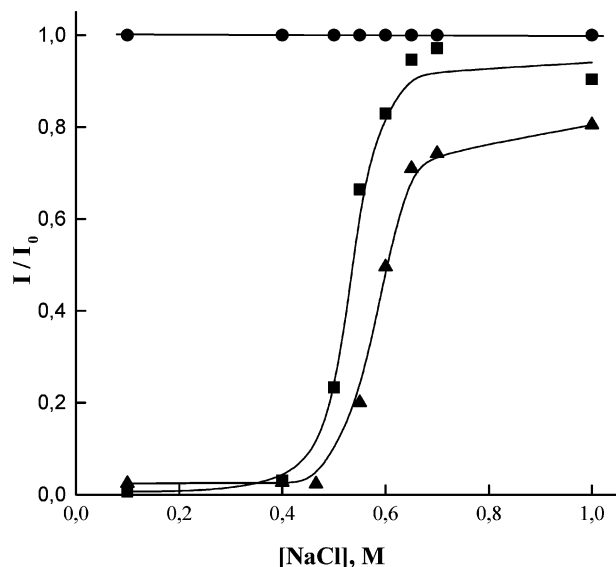


Figure 10. Dependence of relative fluorescence intensity (I/I_0) on NaCl concentration for PMA*Na (●, circles), PMA*Na/PS-*b*-PEVP (▲, triangles), and (3) PMA*Na/PEVP (■, squares) mixtures. [PEVP] = 0.005 base·mol/L; $Z = 0.25$; $\lambda_{\text{ex}} = 342$ nm; $\lambda_{\text{em}} = 375$ nm; pH 9; $\text{DP}_w(\text{PMA}^*\text{Na}) = 2300$.

the swelling of the IPEC particles upon the decrease of the ionic strength of the solution becomes greater.

Disintegration of IPEC at High Concentration of Salt. The pyrene-labeled PMA*Na was used to assess the effect of the added salt on the stability of the IPECs. As discussed above, in the PMA*Na/PS-*b*-PEVP IPEC the fluorescence of the label was completely quenched. However, there was a sharp increase of the fluorescence in a narrow interval of NaCl concentrations above 0.5 M (Figure 10). No alteration in the fluorescence of the free PMA*Na was observed in the same salt concentration range. The behavior observed for PMA*Na/PS-*b*-PEVP IPEC is typical for cooperative disintegration of the IPECs due to screening the electrostatic interactions of the polyions by the added salt.² The disintegration of the IPEC formed between PMA*Na and the homopolymer PEVP was observed in practically the same concentration range of the salt, which suggests that micelle formation of PS-*b*-PEVP had little if any effect on electrostatic binding of PEVP segments with oppositely charged polyions.

Discussion

This study suggests that cooperative electrostatic binding of PMAA polyanions with the cationic PS-*b*-PEVP micelles in dilute aqueous solutions resulted in either precipitation of insoluble IPEC or formation of stable dispersions of soluble IPEC. The soluble IPEC formed as one of the polyelectrolyte components was in excess. It incorporated only one initial block ionomer micelle, which served as a nucleating particle. No disaggregation, fusion, or flocculation of the initial micelles was observed. Furthermore, binding of the polyanion to the micelle did not affect the structure of the PS core (morphology, effective aggregation number, CMC).

Figure 11 presents a hypothetical structure of such complexes. It contains the PS core, the intermediate water-insoluble layer of ionically bound polyions (the IPEC layer per se), and the external lyophilizing layer of the charged fragments of the polyelectrolyte present in excess. This model satisfies the requirements of (1) the cooperative stabilization of the IPEC (formation of sufficiently long sequences of salt bonds between

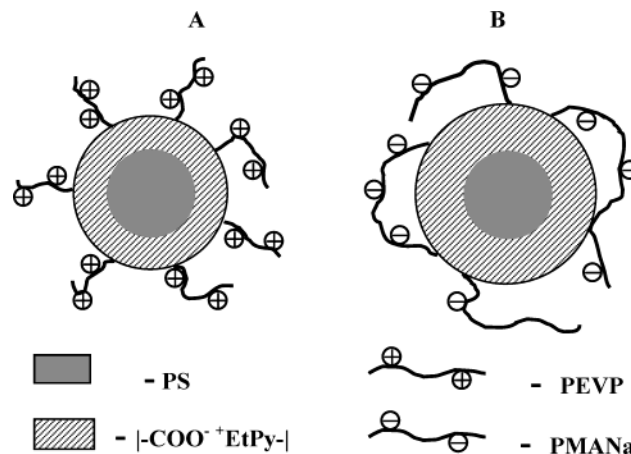


Figure 11. Schematic structure of particles of dispersed (A) positively or (B) negatively charged IPEC PMANa/PS-*b*-PEVP in dilute aqueous solutions. For simplicity small Br^- and Na^+ counterions are not shown.

the polyions) and (2) the stabilization of colloidal particles in dispersion (minimization of hydrophobic surface and formation of external hydrophilic polyelectrolyte layer), which was reinforced by the observation of the polyelectrolyte effect (swelling of the IPEC particles upon the decrease of the ionic strength). This model was analogous to that proposed for soluble PEVP/polyisobutylene-*b*-PMANa complexes formed at excess of the block ionomer.¹⁷ It may also be similar to the structure of complexes of sodium polystyrenesulfonate with PS-*b*-poly-(2-vinylpyridine) micelles in acidic media.¹⁸ However, the latter complexes formed at vast excesses of sodium polystyrenesulfonate and, most likely, were not in equilibrium. To the best of our knowledge there were no reports on soluble, both positively or negatively charged complexes obtained from the same pair of oppositely charged homopolymer and block ionomer. By tuning the ratio between the polymeric components in the solution one can induce thermodynamically reversible transitions between the two types of these complexes. Such IPECs combine in a remarkable way the properties of original block ionomer micelles (CMC, molecular characteristics, morphology) and those of regular IPECs (pH and elementary salt sensitivity).

Analytical and numerical self-consistent-field models were employed to analyze complexes of ionized starlike polymer micelles with oppositely charged polyions.²⁷ This work predicted that the complexes should be electroneutral. It was suggested that the overcharged systems form only under nonequilibrium conditions, for instance, as a result of the “kinetic trapping” of linear polyions in the micelle–polyion aggregates. Our experiment does not support this prediction and demonstrates that (1) there were broad ranges of the compositions of the mixture for which no disproportioning was observed and (2) the soluble complexes contained the excess of one of the polyions. These complexes appeared to be equilibrium since their properties did not depend on the order of mixing of the components. It is noteworthy that the IPECs overcharged by the homopolymer were formed with both long ($\text{DP}_w = 2300$) and short ($\text{DP}_w = 90$) PMANa. The problem of inversion of the charge in the polyelectrolyte complexes is general, has been a subject of intensive theoretical analysis and discussion,²⁸ and is of practical importance for the DNA–polycation IPECs (“polyplexes”) used in gene delivery.^{4,29}

Overall, mixing of the block ionomer micelles with oppositely charged polyelectrolytes provides for a relatively simple tool for the synthesis of a broad range of multilayered polymer–colloidal dispersions that can be used in many areas including

catalysis, biology, medicine, microelectronics, etc. It is hard to overestimate potential possibilities in developing such nano-structured materials, since the practically achievable chemical combinations of the components can be enormous.

Acknowledgment. The authors are grateful for the support of this work provided by National Science Foundation (DMR-0071682), U.S.A., awarded to A.V.K., the Russian Foundation for Basic Research (grant no. 03-03-32161), awarded to E.A.L., the National Science and Engineering Research Council (STR-0181003), Canada, awarded to A.E., and the Russian Science Support Foundation, awarded to E.A.L. We thank Dr. Xing Fu Zhong (McGill University), who synthesized and characterized the block copolymers in connection with other projects, and Ms. Elena Ivleva (Moscow State University), who helped in providing low-angle SLS experiments. We also thank Prof. Alexander Zevin (Moscow State University) for fruitful discussions.

References and Notes

- (1) Smid, J.; Fish, D. Polyelectrolyte Complexes. In *Encyclopedia of Polymer Science and Engineering*; Mark, H. F., Bikales, N. M., Overberger, C. G., Menges, G., Eds.; Wiley: New York, 1988; Vol. 11, p 720.
- (2) Kabanov, V. Fundamentals of Polyelectrolyte Complexes in Solution and the Bulk. In *Multilayer Thin Films*; Decher G., Schlenoff J. B., Eds.; WILEY-VCH: Weinheim, Germany, 2003; p 47.
- (3) Kabanov, V. A. Basic Properties of Soluble Interpolyelectrolyte Complexes Applied to Bioengineering and Cell Transformations. In *Macromolecular Complexes in Chemistry and Biology*; Dubin, P., Bock, J., Davies, R. M., Schulz, D. N., Thies, C., Eds.; Springer-Verlag: Berlin, Germany, 1994; p 151.
- (4) (a) Kabanov, A. V.; Kabanov, V. A. *Bioconjugate Chem.* **1995**, *6*, 7–20. (b) Boussif, O.; Lezoualc'h, F.; Zanta, M. A.; Mergny, M. D.; Scherman, D.; Demeneix, B.; Behr, J. P. *Proc. Natl. Acad. Sci. U.S.A.* **1995**, *92*, 7297–7301. (c) Tang, M.; Szoka, F. *Gene Ther.* **1997**, *4*, 823–832.
- (5) Selb, J.; Gallot, Y. Ionic Block Copolymers. In *Developments in Block Copolymers*; Goodman I., Ed.; Elsevier Applied Science: London, UK, 1985; Vol. 2, p 27.
- (6) Zhang, L.; Khougaz, K.; Moffitt, M.; Eisenberg, A. Self-Assembly of Block Polyelectrolytes. In *Amphiphilic Block Copolymers: Self-Assembly and Applications*; Alexandridis P., Lindman B., Eds.; Elsevier: Amsterdam, The Netherlands, 2000; p 87.
- (7) Kabanov, A. V.; Bronich, T. K.; Kabanov, V. A.; Yu, K.; Eisenberg, A. *Macromolecules* **1996**, *29*, 6797–6802.
- (8) (a) Gohy, J.-F.; Varshney, S. K.; Antoun, S.; Jérôme R. *Macromolecules* **2000**, *33*, 9298–9305. (b) Gohy, J.-F.; Varshney, S. K.; Antoun, S.; Jérôme, R. *Macromolecules* **2001**, *34*, 2745–2747.
- (9) (a) Harada, A.; Kataoka K. *Macromolecules* **1995**, *28*, 5294–5299. (b) Gohy, J.-F.; Varshney, S. K.; Jérôme, R. *Macromolecules* **2001**, *34*, 3361–3366.
- (10) (a) Bronich, T. K.; Kabanov, A. V.; Kabanov, V. A.; Yu, K.; Eisenberg, A. *Macromolecules* **1997**, *30*, 3519–3525. (b) Kabanov, A. V.; Bronich, T. K.; Kabanov, V. A.; Yu, K.; Eisenberg, A. *J. Am. Chem. Soc.* **1998**, *120*, 9941–9942. (c) Bronich, T. K.; Cherry, T.; Vinogradov, S. V.; Eisenberg, A.; Kabanov, V. A.; Kabanov, A. V. *Langmuir* **1998**, *14*, 6101–6106. (d) Bronich, T. K.; Popov, A. M.; Eisenberg, A.; Kabanov, V. A.; Kabanov, A. V. *Langmuir* **2000**, *16*, 481–489. (e) Bronich, T. K.; Solomatin, S. V.; Yaroslavov, A. A.; Eisenberg, A.; Kabanov, V. A.; Kabanov, A. V. *Langmuir* **2000**, *16*, 4877–4881.
- (11) (a) Kabanov, A. V.; Vinogradov, S. V.; Suzdaltseva, Yu. G.; Alakhov, V. Yu. *Bioconjugate Chem.* **1995**, *6*, 639–643. (b) Wolfert, M. A.; Schaht, E. H.; Tonceva, V.; Ulbrich, K.; Nazarov, O.; Seymour, L. W. *Hum. Gene Ther.* **1996**, *7*, 2123–2133. (c) Kataoka, K.; Togawa, H.; Harada, A.; Yasugi, K.; Matsumoto, T.; Katayose, S. *Macromolecules* **1996**, *29*, 8556–8557. (d) Choi, Y. H.; Liu, F.; Kim, J. S.; Choi, Y. K.; Park, J. S.; Kim, S. W. *J. Controlled Release* **1998**, *54*, 39–48. (e) Bronich, T. K.; Nguyen, H.-K.; Eisenberg, A.; Kabanov, A. V. *J. Am. Chem. Soc.* **2000**, *120*, 8339–8343.
- (12) (a) Harada, A.; Kataoka, K. *Macromolecules* **1998**, *31*, 288–294. (b) Harada, A.; Kataoka, K. *Langmuir* **1999**, *15*, 4208–4212.
- (13) (a) Astafieva, I.; Zhong, X.-F.; Eisenberg A. *Macromolecules* **1993**, *26*, 7339–7352. (b) Astafieva, I.; Khougaz, K.; Eisenberg, A. *Macromolecules* **1995**, *28*, 7127–7134. (c) Khougaz, K.; Astafieva, I.; Eisenberg, A. *Macromolecules* **1995**, *28*, 7135–7147.
- (14) (a) Guenoun, P.; Davis, H. T.; Tirrell, M.; Mays, J. W. *Macromolecules* **1996**, *29*, 3965–3969. (b) Procházka, K.; Martin, T. J.; Munk, P.; Webber, S. E. *Macromolecules* **1996**, *29*, 6518–6525. (c) Szczubialka, K.; Ishikawa, K.; Morishima, Y. *Langmuir* **1999**, *15*, 454–462. (d) Schuch, H.; Klingler, J.; Rossmannith, P.; Frechen, T.; Gerst, M.; Feldthusen, J.; Müller, A. H. E. *Macromolecules* **2000**, *33*, 1734–1740. (e) Gohy, J.-F.; Creutz, S.; Garcia, M.; Mahltig, B.; Stamm, M.; Jérôme, R. *Macromolecules* **2000**, *33*, 6378–6387.
- (15) Lysenko, E. A.; Bronich, T. K.; Eisenberg, A.; Kabanov, V. A.; Kabanov, A. V. *Macromolecules* **1998**, *31*, 4511–4515.
- (16) Lysenko, E. A.; Bronich, T. K.; Slonkina, E. V.; Eisenberg, A.; Kabanov, V. A.; Kabanov, A. V. *Macromolecules* **2002**, *35*, 6351–6361.
- (17) (a) Pergushov, D. V.; Remizova, E. V.; Feldthusen, J.; Zevin, A. B.; Müller, A. H. E.; Kabanov, V. A. *J. Phys. Chem. B* **2003**, *107*, 8093–8096. (b) Pergushov, D. V.; Remizova, E. V.; Gradielski, M.; Lindner, J.; Feldthusen, J.; Zevin, A. B.; Müller, A. H. E.; Kabanov, V. A. *Polymer* **2004**, *45*, 367–378.
- (18) Talingting, M. R.; Voigt, U.; Munk, P.; Webber, S. E. *Macromolecules* **2000**, *33*, 9612–9619.
- (19) Gauthier, S.; Eisenberg, A. *Macromolecules* **1987**, *20*, 760–767.
- (20) Gauthier, S.; Duchesne, D.; Eisenberg, A. *Macromolecules* **1987**, *20*, 753–759.
- (21) Pavlova, N. R.; Kirsh, Yu. E.; Kabanov, V. A. *Polym. Sci. U.S.S.R.* **1979**, *21*, 2276–2283 (translated from *Vysokomol. Soed. Ser. A* **1979**, *21*, 2062–2069).
- (22) Lipatov, Yu. S.; Zubov, P. N. *Vysokomol. Soed. Ser. A* **1959**, *1*, 88–93.
- (23) Krakovyak, M. G.; Anufrieva, E. V.; Skorokhodov, S. S. *Polymer Science U. S. S. R.* **1969**, *11*, 2842–2846. (Translated from *Vysokomol. Soedin. Ser. A* **1969**, *11*, 2499–2503).
- (24) Izumrudov, V. A.; Zevin, A. B. *Polym. Sci. U.S.S.R.* **1976**, *18*, 2840–2846 (translated from *Vysokomol. Soedin. Ser. A* **1976**, *18*, 2488–2494).
- (25) Nagasawa, M. *Pure Appl. Chem.* **1971**, *26*, 519–536.
- (26) Bakeev, K. N.; Izumrudov, V. A.; Kuchanov, S. I.; Zevin, A. B.; Kabanov, V. A. *Macromolecules* **1992**, *25*, 4249–4254.
- (27) Simmons, C.; Webber, S. E.; Zhulina, E. B. *Macromolecules* **2001**, *34*, 5053–5066.
- (28) Nguyen, T. T.; Grosberg, A. Yu.; Shklovskii, B. I. *J. Chem. Phys.* **2000**, *113*, 1110–1125.
- (29) Kabanov, A. V.; Bronich, T. K. Structure, dispersion stability and dynamics of DNA and polycation complexes. In *Pharmaceutical Prospective of Nucleic Acid-Based Therapeutics*; Kim, S. W., Machato, R., Eds.; Taylor & Francis: New York, 2002; p 164.